



ISSN: 0067-2904

The Numerical Analysis for Electrical Streamer Discharge Behaviour in Transformer Oil

Ali F. Al-rawaf^{1,2*}, Thamir H. Khalaf¹

¹ Department of Physics, College of Science, University of Baghdad, Baghdad, Iraq

² Department of Anesthesia Techniques, AlSafwa University College, Karbala, Iraq

Received: 8/12/2021

Accepted: 1/5/2022

Published: 30/1/2023

Abstract

In this paper, a numerical analysis was carried out using finite element method to analyse the mechanisms for streamer discharges. The hydrodynamic model was used with three charge carriers equations (positive ion, negative ion and electron) coupled with Poisson equation to simulate the dynamic of streamer discharge formation and propagation. The model was tested within a 2D axisymmetric tip-plate electrodes configuration using the transformer oil as the dielectric liquid. The distance between the electrodes was fixed at 1 mm and the applied voltage was 130 kV at 46 ns rising time. Simulation results showed that the time has a clear effect on the streamer propagation along the symmetry axis. In addition, it was observed that the highest value of the voltage was recorded at 46 ns and the minimum voltage required for insulation breakdown was 112 kV at 200 ns. It was revealed that the streamer velocity recorded the highest value when the streamer reaches the plate electrode and the lowest value when the streamer begins to propagate. Results also showed that the streamer discharge was dominated by positive ions while the negative ions have a low effect.

Keywords: Streamer discharge, COMSOL Multiphysics, transformer oil, space charge density, positive and negative ions.

التحليل العددي لسلوك التفريغ الكهربائي الخيطي في زيت المحولات

علي فاضل الرواف^{1,2*}, ثامر حميد خلف²

¹ قسم الفيزياء، كلية العلوم، جامعة بغداد، محافظة بغداد، العراق

² قسم تقنيات التخدير، كلية الصفوة الجامعة، محافظة كربلاء، العراق

الخلاصة

في هذا البحث تم إجراء تحليل عددي باستخدام طريقة العناصر المحدودة لتحليل آليات التفريغ الخيطي. تم استخدام النموذج الهيدروديناميكي مع ثلاث معادلات حاملات شحنة (الايونات الموجبة والايونات السالبة والالكترونات) التي تقترن بمعادلة بوسون لمحاكاة ديناميكية التفريغ الخيطي وانتشاره. تم اختبار هذا النموذج ضمن تكوين قطب كهربائي ذو لوحة إبرة ثنائية الأبعاد باستخدام زيت المحولات كسائل عازل. تم

*Email: ali.mohammed1104@sc.uobaghdad.edu.iq

تثبيت المسافة بين الأقطاب الكهربائية عند 1 مم وثبت الجهد المطبق عند 130 كيلو فولت بوقت زمن النهوض 46 نانوثانية. أظهرت نتائج المحاكاة أن للزمن تأثير واضح على انتشار التفريغ الخيطي على طول محور التناظر. بالإضافة إلى ذلك ، تم تسجيل أعلى قيمة للجهد في وقت قدره 46 نانوثانية ولوحظ ان الحد الأدنى للجهد المطلوب لانهايار العزل هو 112 كيلو فولت عند زمن 200 نانوثانية. وجد ايضا أن أعلى قيمة لسرعة الغاسل يتم تسجيلها عندما يصل تفريغ الخيطي إلى القطب الأرضي وأقل قيمة عندما يبدأ التفريغ الخيطي بالانتشار من قطب الانود. كما أوضحت نتائج المحاكاة ايضا أن تفريغ الخيطي يغلب عليه تركيز الايونات الموجبة بينما الايونات السالبة كانت أقل تأثيرا.

1. Introduction

The electric discharge phenomenon is very complex and is determined by various environmental variables such as the chemical composition and purity of the medium, the magnitude and polarity of the applied voltage. It is difficult to capture this complex discharge process in detail in an experimental approach. Therefore, recently, many researchers have proposed various methodologies using numerical analysis techniques to analyze the electric discharge phenomenon [1-5]. To develop such a numerical analysis technique, the discretization method using the finite element method (FEM) has been applied. The FEM is widely used in the numerical solution of electric field problems. Unlike other numerical methods, FEM is a very general method and is, therefore, a versatile tool for solving a wide range of electric field problems. The principle of this method is to divide the field of study into several finite elements (called mesh). This is a very important step since the choice of the shape of the mesh element is essential in the accuracy of the results obtained. It is therefore necessary to find its form and its degree of approximation, which are the most suitable for the geometry of the field of study [6]. As the multiphysics analysis technology has been greatly developed, various attempts to analyze the discharge phenomenon system using the analysis tool has been proposed.

The characteristics of streamer in transformer oil including effects of various voltage magnitude, geometry, gap, polarity and speed were studied by Abdulla et al. [7] Lesaint et al. [8], Linhjell et al. [9], Bhatt et al.[10], Zhou et al. [11] and Salazar et al. [12]. Jadidian [13] simulated space charge transportation and breakdown mechanism of the steamer discharge. The impacts of electrode structure and the characteristics of the insulation liquid on the propagation of streamer were briefed by Sun et al.[2] and Bruggeman et al. [14].

This paper focuses on the mechanism of streamer discharge phenomena which is explained using a numerical analysis technique that can be applied to the liquid discharge problem. Numerical analysis was applied within a two-dimensional tip-plate configuration of electrodes, and quantitatively analyzed for the initiation and propagation of streamer discharge. COMSOL commercial software based on the finite element method was used to construct and solve such a multiphysics environment numerically.

2. Streamer Discharge Analysis Model

2.1. Governing Equations

To describe the formation and development of streamer discharge in the dielectric liquid, the hydrodynamic equation was introduced, which expresses the charge continuity equation for electrons, positive ions and negative ions, and the Poisson equation for electric fields as follows[15]:

$$\nabla \cdot (\varepsilon \vec{E}) = \rho_e + \rho_p + \rho_n \quad (1)$$

$$\frac{\partial \rho_p}{\partial t} + \nabla \cdot (\rho_p \mu_p \vec{E}) = G_F(|\vec{E}|) + \frac{\rho_p \rho_e R_{pe}}{q} + \frac{\rho_p \rho_n R_{pn}}{q} \quad (2)$$

$$\frac{\partial \rho_n}{\partial t} - \nabla \cdot (\rho_n \mu_n \vec{E}) = \frac{\rho_e}{\tau_a} - \frac{\rho_p \rho_n R_{pn}}{q} \quad (3)$$

$$\frac{\partial \rho_e}{\partial t} - \nabla \cdot (\rho_e \mu_e \vec{E}) = -G_F(|\vec{E}|) - \frac{\rho_p \rho_e R_{pe}}{q} - \frac{\rho_e}{\tau_a} \quad (4)$$

Here, ε is the dielectric constant, E is the electric field, q is the electric charge, $G_F (|E|)$ is the ionization source term in the insulating fluid that responds to the electric field, R_{pe} and R_{pn} are the recombination rate constants of ions-electrons and ions- ions in the insulating fluid, τ_a is the attachment time, and ρ_e , ρ_p , and ρ_n are the densities for electrons, positive ions, and negative ions, respectively [15, 16].

When no external voltage is applied, molecules in an insulating fluid share electrons and are in a stable state. When these neutral molecules are affected by a strong electric field, they lose their outermost electrons, become charged, and are separated into positive ions and free electrons. The ion source term of the electric charge responding to a high electric field is expressed as a charge density ratio based on the electron tunneling action of the dielectric and is applied to the Zener ionization model [15, 17, 18].

$$G_F(|\vec{E}|) = \frac{q^2 n_0 a |\vec{E}|}{h} \exp\left(-\frac{\pi^2 m^* a \Delta^2}{q h^2 |\vec{E}|}\right) \quad (5)$$

Where n_0 is the density number of molecules that can be ionized, a is the molecular separation constant, m^* is the effective mass in the insulating fluid, h is Planck constant, and Δ is the ionization energy of the molecule. In the case of molecular ionization, many chemical reactions are involved, but this paper is limited to the mechanism of generating two free charges by separating neutral molecules, reacting under the influence of an electric field, into positive ions and electrons. The main physical parameters required in the simulation process in this paper were taken from the literature [13, 19], as shown in Table 1.

Table 1: The parameters used in the simulations [13, 19]

Parameter	Meanings	Value
n_0	Density number of molecules	$1 \times 10^{23} \text{ m}^{-3}$
a	Molecular separation constant	$3.0 \times 10^{-10} \text{ m}$
m^*	Effective electron mass	$9.11 \times 10^{-32} \text{ kg}$
R_{pn}, R_{pe}	Recombination rate constants of ions-electrons and ions- ions in the insulating fluid	$1.64 \times 10^{-17} \text{ m}^3 \text{ s}^{-1}$
μ_p, μ_n	Mobility of positive and negative ions	$1 \times 10^{-9} \text{ m}^2 \text{ V}^{-1} \text{ s}^{-1}$
μ_e	Mobility of electrons	$1 \times 10^{-4} \text{ m}^2 \text{ V}^{-1} \text{ s}^{-1}$
Δ	Ionization energy of the molecule	8.5 eV
τ_a	Electron attachment time	200 ns

2.2. Computational Domain

The numerical analysis model was modeled as a tip-plate electrode arrangement based on IEC 60897 Standard [20] with a 1 mm void as shown in Figure 1(a). The analysis model was calculated by setting it as 2D axisymmetric. The tip of the pin was designed to have a radius

of curvature of $40 \mu\text{m}$ and the area which was used to calculate the electric field was set to $r \times z = 2 \times 2 \text{ mm}^2$.

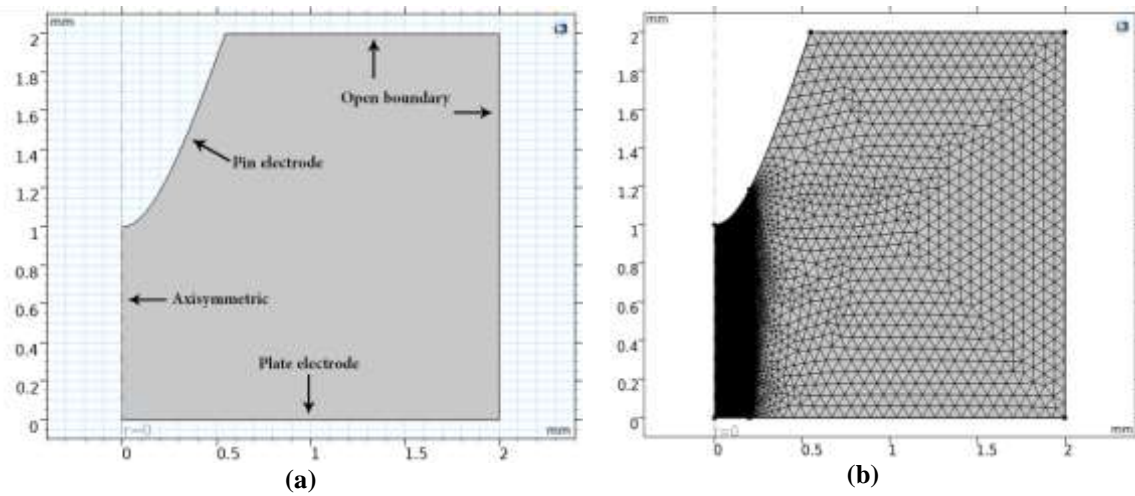


Figure 1: (a) 2D axial symmetric diagram (b) The area in COMSOL (c) mesh map area

The initial distribution of electrons and positive ions is concentrated around the tip electrode and in the region close to the symmetry line. Therefore, to improve the convergence of the numerical analysis, the finite element network was intensively applied around the tip electrode and in the symmetry line as shown in Figure 1(b). Figure 2 shows the zoom of the mesh and the accuracy of this model's entanglement through some meshes. The accurate entanglement is considered a guarantee of model convergence in numerical calculations.

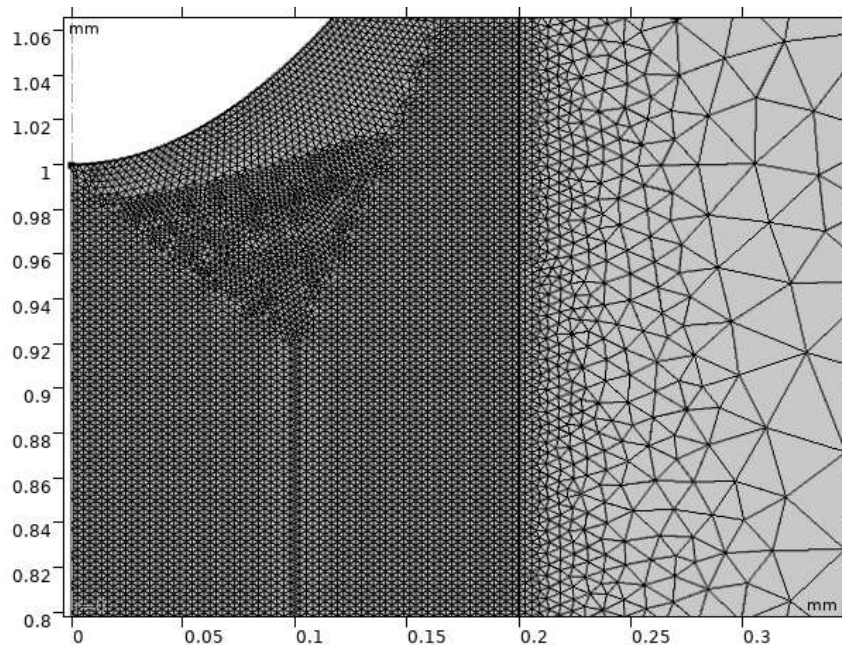


Figure 2: Zoom of the mesh map area in COMSOL

2.3. Boundary Condition and Numerical Algorithm

Once geometry was introduced into the COMSOL Multiphysics, the spatial and boundary conditions for the equations of the model must be defined. For the Poisson Equation (1) describing the electrostatic process, the plate type electrode potential was set to ground, $V=0$, and the pin type electrode potential was set to $V=V_i$ and the zero charge boundary condition

was applied to the insulated walls. The insulating walls are not affected by the lines of the electric fields. The voltage applied to the pin type electrode is defined by subtracting two exponential functions that generate the standard lightning strike voltage according to IEC 600060-1 [21] as:

$$V_i = KV_0 \left(e^{-\frac{t}{\tau_1}} - e^{-\frac{t}{\tau_2}} \right) \quad (6)$$

Where K is a dimensionless compensation factor intended to maintain maximum value of the percussion and is approximately equal to V_0 , in general, the maximum value resulting from subtracting two exponential functions is not necessarily equal to one [22], τ_1 the rising time and τ_2 the falling time. Figure 3 shows the waveform of IEC 600060-1 lighting impulse in this simulation. It is observed that the voltage gradually increases with time until it reaches its highest value (130 kV) at 46 ns, and then begins to decrease gradually to reach its lowest value (112 kV) at 200 ns.

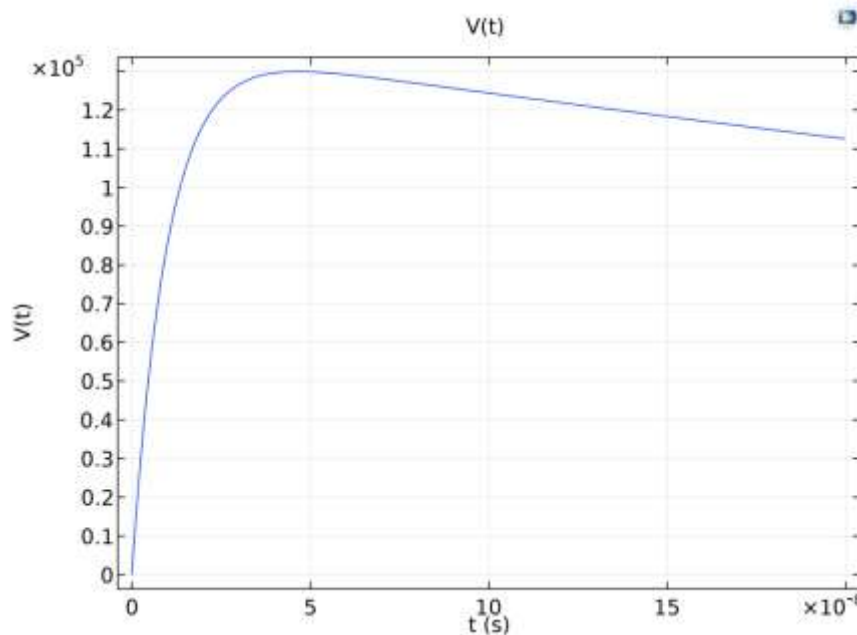


Figure 3: The wavelength of lighting impulse voltage in simulation

For the three-carrier continuity Equations (2-4), both the plate type electrode potential and the pin type electrode potential were set to the outflow boundary conditions, and the outer boundary was set with no flux boundary conditions. Commercial computation software COMSOL Multiphysics version 5.6 was employed to solve the hydrodynamic model of the streamer discharge. The modules including “Electrostatic” and “Transport of Diluted Species” were used to solve Poisson’s Equation (1) and carrier continuity Equations (2-4).

1.3 Results and Discussion

The insulation of the IEC 60897 model was assumed to be pure transformer oil, and when a strong electric field is applied from the outside, a positive polarity streamer occurs. When the electric field is concentrated on the tip electrode, an unequal electric field is formed from the tip-plate electrode structure and leads to the streamer channel. When the applied electric field exceeds 10^6 - 10^8 [V/m], free electrons are emitted from the electrode and it leads to ionization, dissociation, recombination, and electron adhesion that collide with neutral particles. Figure 4 shows the electric field distribution within 1 mm gap distance at different instants. It was observed that time has a clear effect on the propagation and development of

the streamer discharge towards the ground plate. Through Figure 4 (a), it is seen that the electric field occupies its highest value at 46 ns. This is due to the fact that the value of the applied voltage at this instant occupies the higher value, as mentioned in the previous section. Furthermore it was noticed that the streamer discharge is onset to grow and flow slightly towards the symmetry axis. The propagation and development of the streamer discharge are shown clearly in the axial direction of the symmetry line in Figure 4 (b) and (c). When a streamer discharge is in contact with the cathode at 200 ns, the electric field will rapidly be redistributed, and a large number of electrons and ions will be generated near the cathode as shown in Figure 4 (d). The shape and stability of the streamer at this time has changed when it reached the ground electrode. This indicates that the streamer discharge has reached the breakdown point. From the previous experimental results, it was reported that positive streamers propagate linearly from the high electric field region of the tip electrode to the low electric field region, and the negative discharge propagates radially from the center of the high electric field region [23-26].

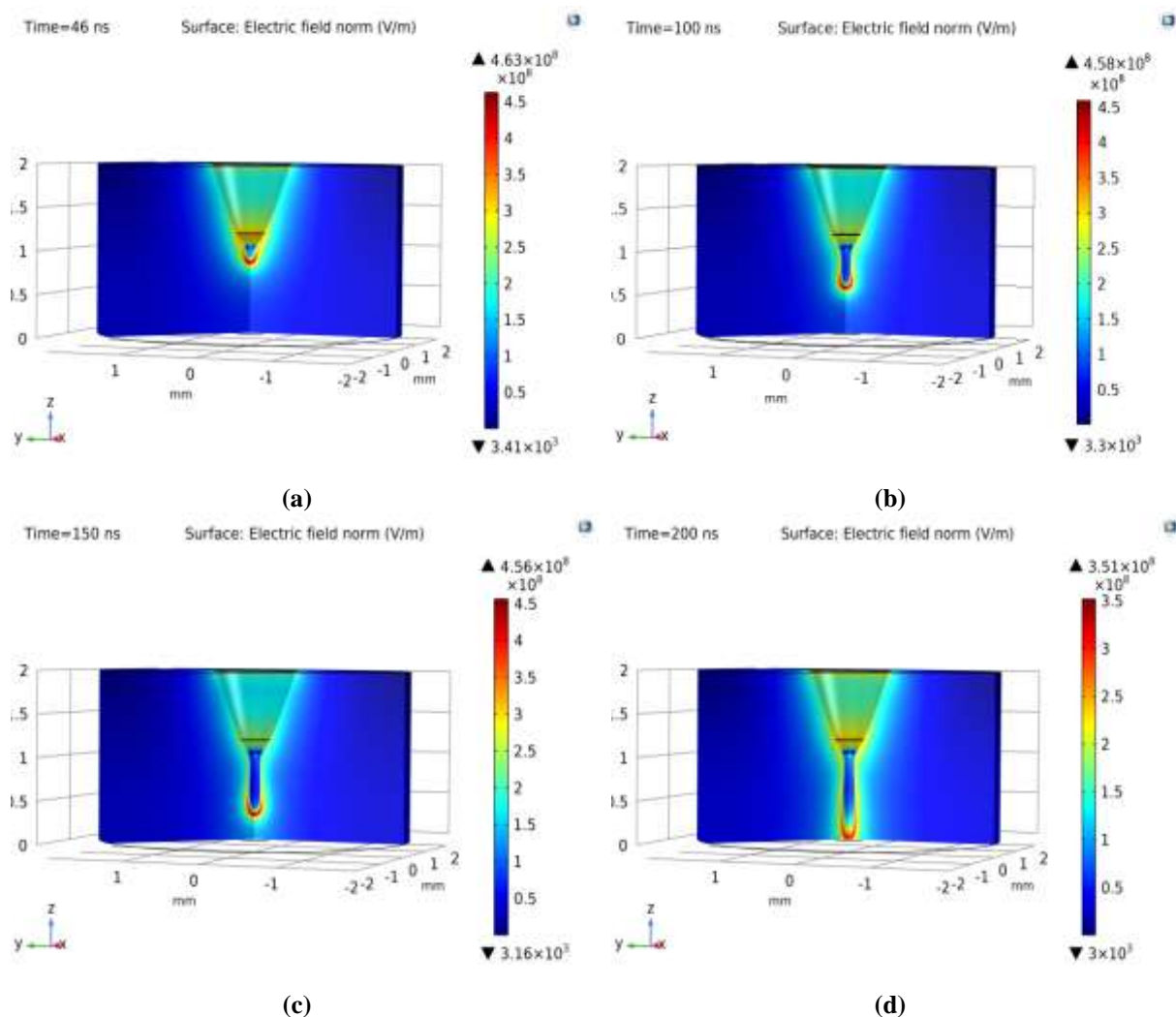


Figure 4: Streamer discharge development within different times in transformer oil (a) 46 ns (b) 100 ns (c) 150 ns (d) 200 ns

Figure 5 shows the propagation of the electric field with time. The maximum electric field appears in the head of the streamer, and the electric field reaches 4.63×10^8 V/m at 46 ns before the streamer penetrates the plate electrode. During the development of streamer discharge, it was found that the field strength remained roughly constant at 4.63×10^8 ,

4.58×10^8 , and 4.56×10^8 V/m under 46, 100, and 150 ns, respectively. This roughly constant electric field strength maintains the stability of the highly coupled processes of streamer discharge propagation, which are caused by background molecules ionization and charged carriers' motion under the high electric field. According to the simulation, this electric field's magnitude is similar to the one observed in the experiment at the front of the streamer discharge as shown in [18]. The value of the applied voltage is 112 kV when the streamer discharge reaches the ground electrode, where it was found that the electric field decreased significantly at this point. The reason for the sudden decrease in the electric field is a result of the arrival of the streamer to the ground electrode, which leads to a voltage breakdown. In addition, the contact of the streamer discharge with the ground surface leads to the accumulation of the density of charges on the surface. Due to this accumulation on the ground surface, a decrease in density occurs, which, in turn, reduces the electric field value. According to Poisson's law, the density of the charges is closely related to the electric field. The breakdown voltage can be defined as the lowest voltage required for the streamer to reach the ground electrode and thus the occurrence of breakdown[15].

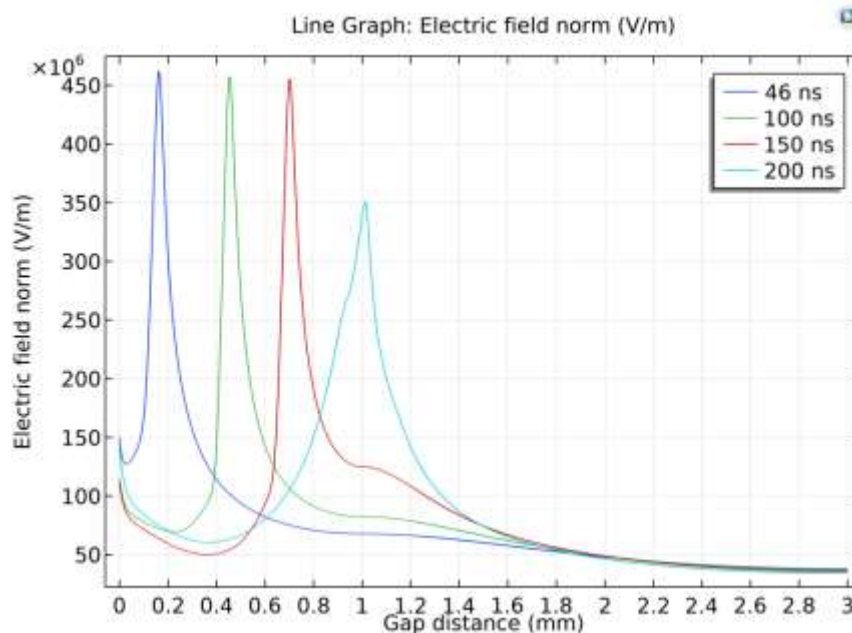


Figure 5: Distribution of electric field along axisymmetric at different instant

One of the important parameters to study the streamer discharge behavior is the speed of this streamer. The velocity of the streamer can be measured by knowing the length of the streamer tip at a given time. Figure 6 shows the position of streamer discharge tip at various instants. From the figure, it is found that increasing the time, increases the streamer length towards the ground electrode. The highest value of streamer velocity was recorded at 5 Km/s when the streamer reached the ground electrode, and the lowest value was recorded at 4 Km/s when the streamer started to propagate. Through comparison with the experimental results of previous works in [22], it was confirmed that the average electric field propagation speed was about 5.4 Km/s. This is in agreement with the results of the numerical analysis and similar to the experimental results of Jadidian et al.[27-29].

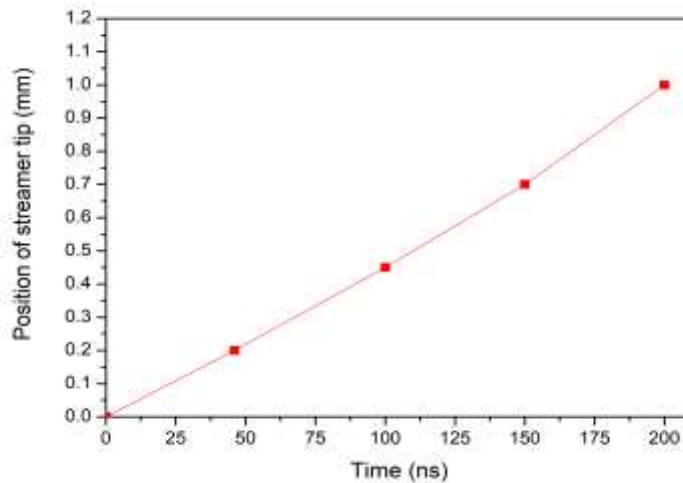


Figure 6: Position of streamer discharge tip at various instants.

Figure 7 shows the numerical results of the initiation and propagation process of the streamer discharge at the tip electrode. Through the analysis results, it can be seen that the space charge distribution propagates linearly with time from the tip electrode to the plate electrode. This behaviour of space charge density is confirmed to be in good agreement with the experimental and numerical results value in previous studies [30, 31].

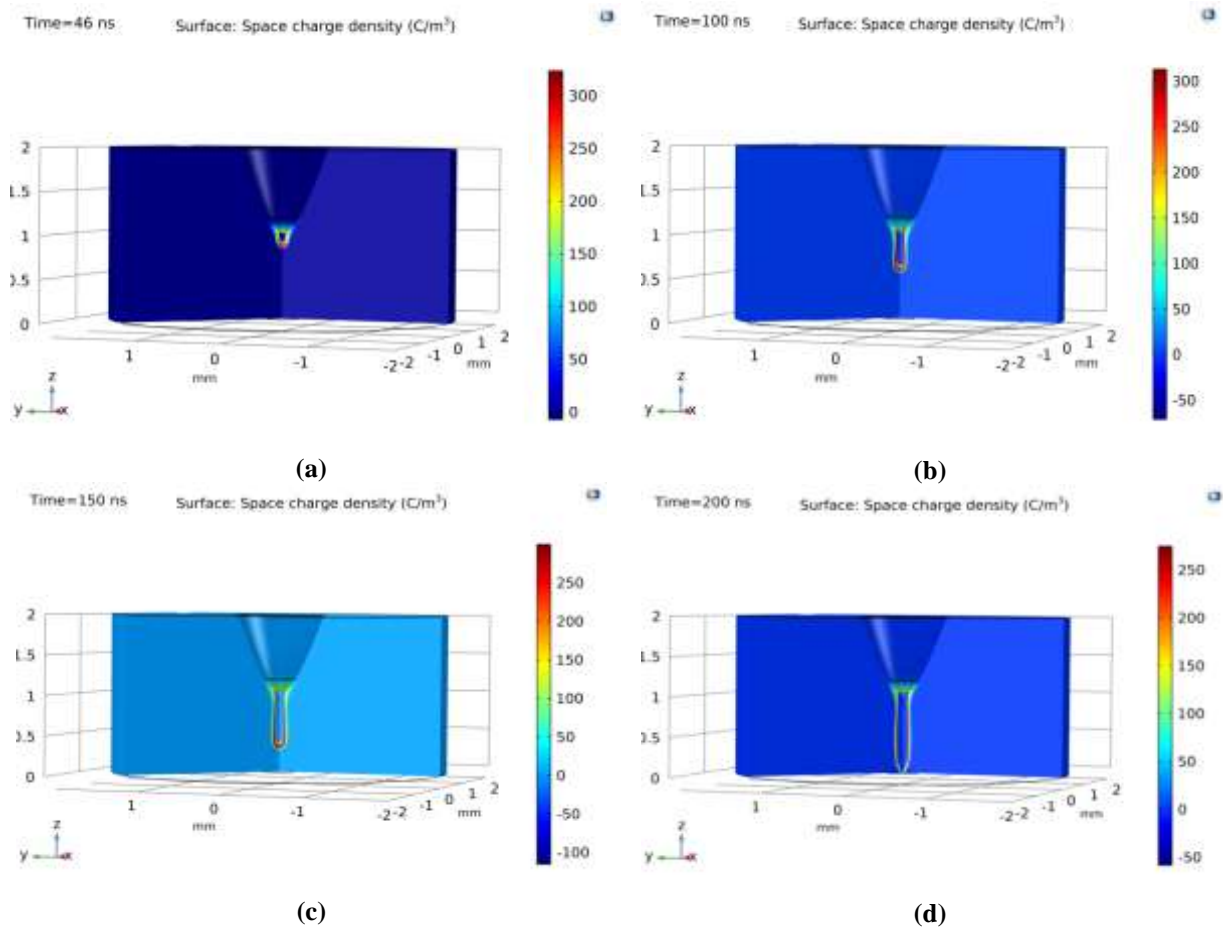


Figure 7: Space charge density within different times (a) 46 ns (b) 100 ns (c) 150 ns (d) 200 ns

The process and morphology of the positive ions, negative ions and electrons starting at the tip of the tip and progressing to the plate electrode are clearly observed in Figures 8, 9 and 10, respectively. The effect of time is clearly observed on the development of the streamer discharge. When the streamer discharge is connected to the plate electrode, it can be seen that the shape of the streamer discharge and its value have clearly changed.

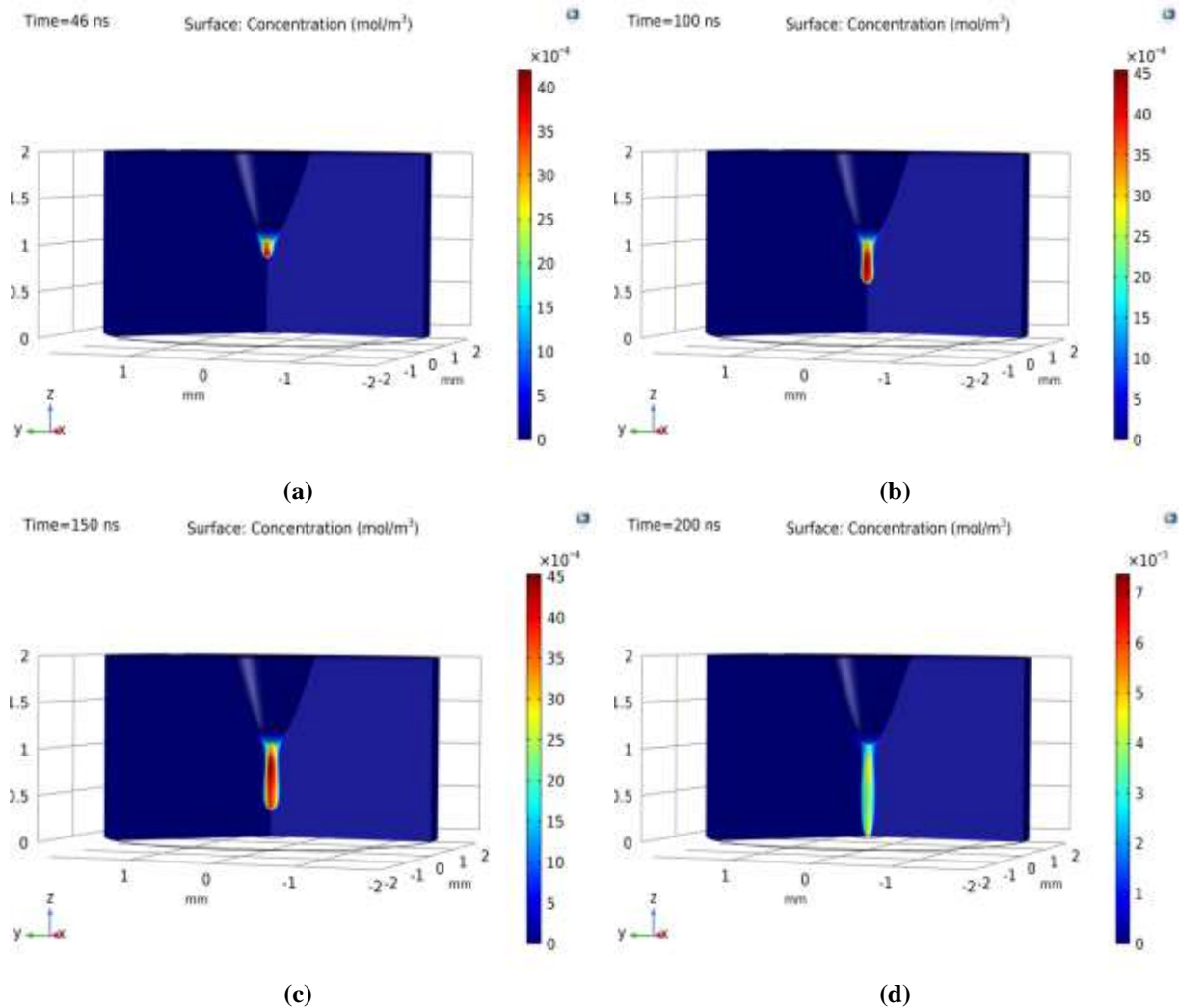


Figure 8: Distribution of positive ion concentrations within different times (a) 46 ns (b) 100 ns (c) 150 ns (d) 200 ns

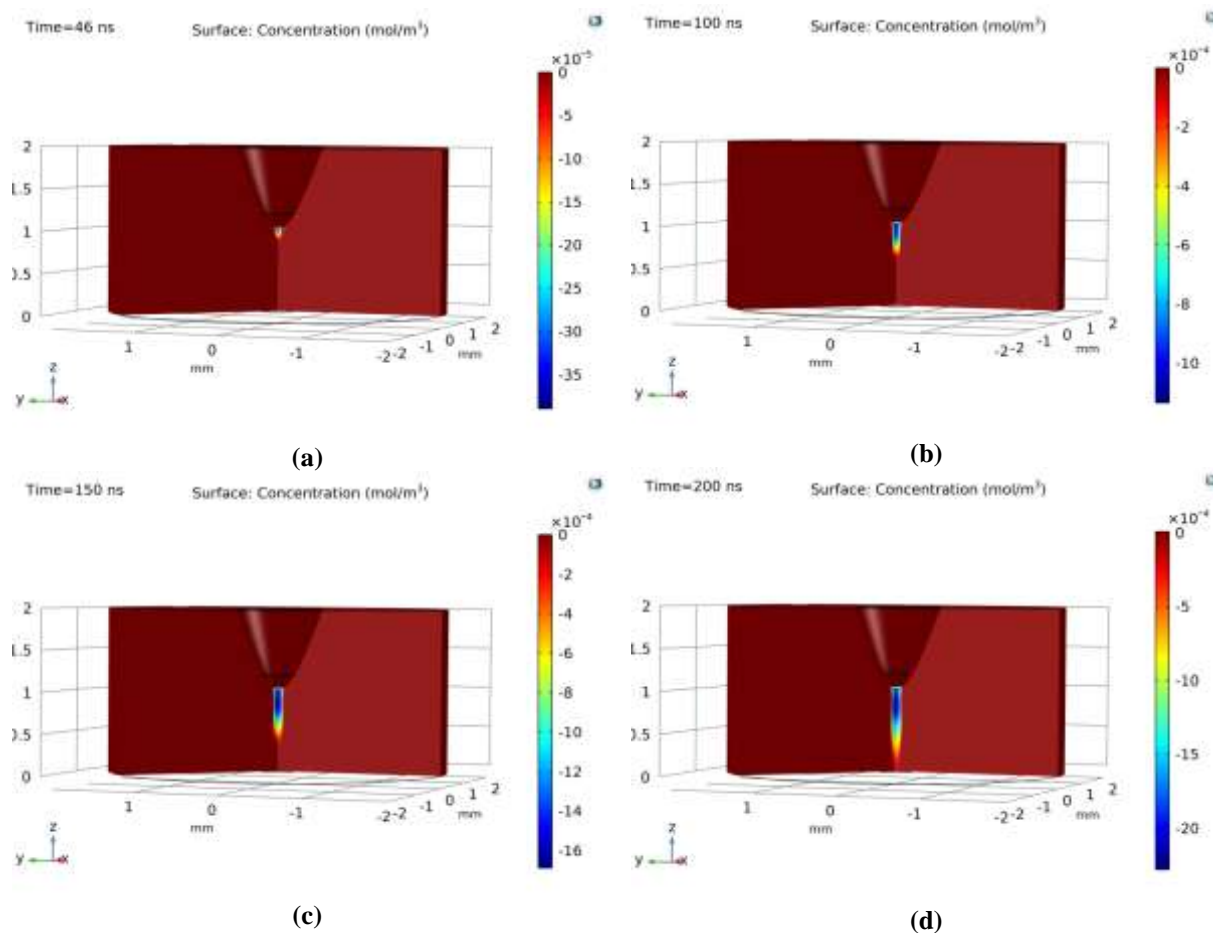


Figure 9: Distribution of negative ion concentrations within different times (a) 46 ns (b) 100 ns (c) 150 ns (d) 200 ns

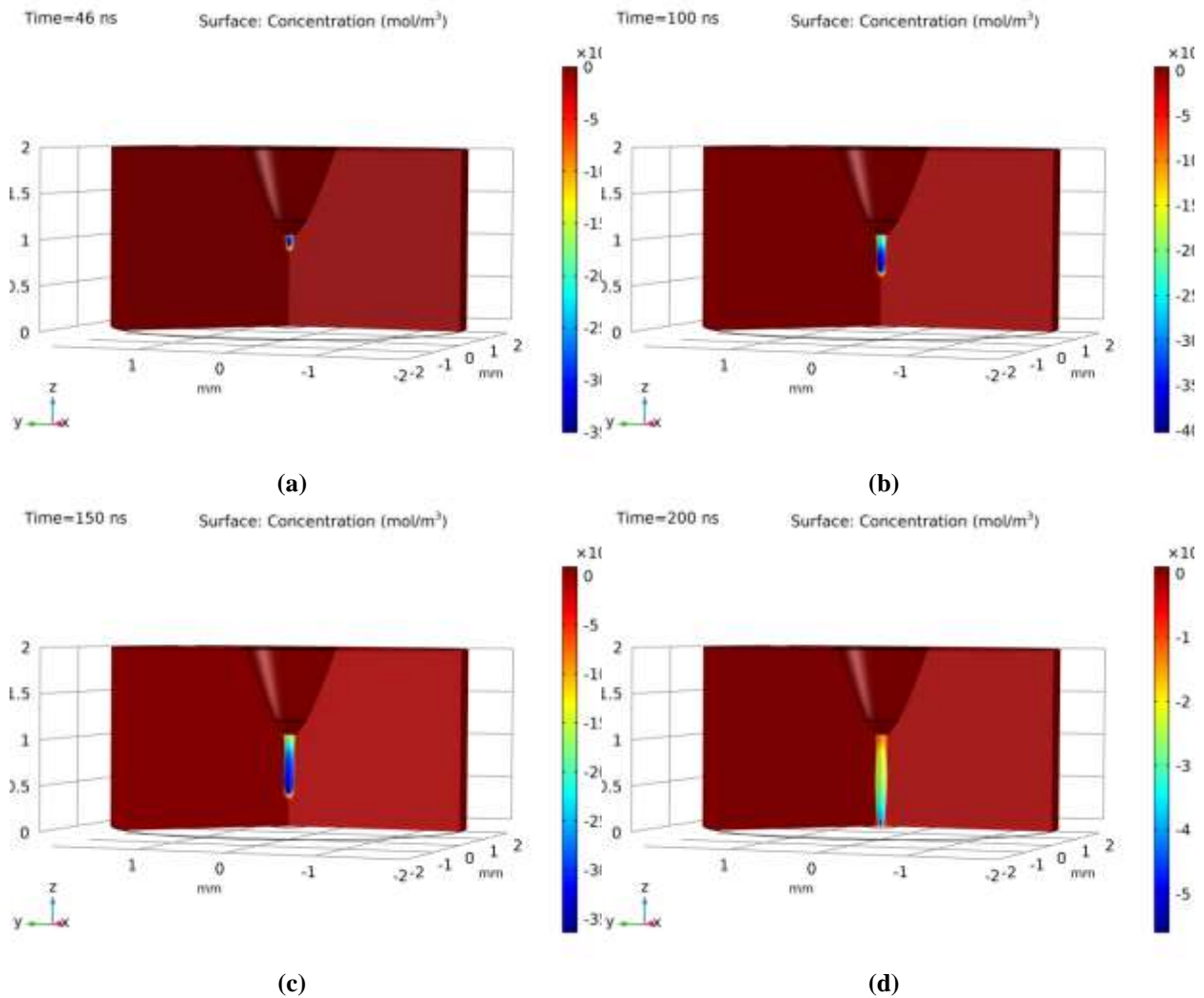


Figure 10: Distribution of electron density concentrations within different times (a) 46 ns (b) 100 ns (c) 150 ns (d) 200 ns

Figure 11 shows the distributions of concentrations for positive ions densities, negative ions densities, and electrons densities according to time in streamer discharge. In Figure 11 (a), it can be seen that the value of positive ion concentration within 46 ns begins to rise in a certain range, then decreases and finally rises to reach the value of 0.0042 mol/m^3 . This condition is repeated at 100 and 150 ns to reach the highest values of 0.0041 mol/m^3 and 0.0038 mol/m^3 , respectively. A sudden rise is shown in the value of the positive ion concentration when the time reaches 200 ns. This increase is normal because the connection of the streamer discharge to the ground electrode leads to the creation of a channel rich in positive ions between the two electrodes, and this in turn leads to the process of liquid breakdown. During the process of the streamer, the positive ions stay along the axisymmetric between the electrodes because of their low mobility compared with electrons. Negative ions are generated by the attachment mechanism when the electrons generated by the molecular ionization mechanism are traveling from the streamer discharge heading towards the positive tip high voltage electrode. Hence, as seen in Figure 11 (b), negative ion densities at different time instances are smaller than positive ion and electron densities as depicted in Figures 11 (a) and (c). High mobility electrons and negative ions are swept away from the ionization zone and absorbed by the ground electrode and due to this, the value of the electrons and negative ions becomes very low. Finally, from the analysis results, it can be seen that positive

ions propagate from the anode to the cathode, and electrons are generated by ionization, but the negative ions are concentrated around the anode. Therefore, from the results, it can be seen that the streamer discharge is dominated by positive ions.

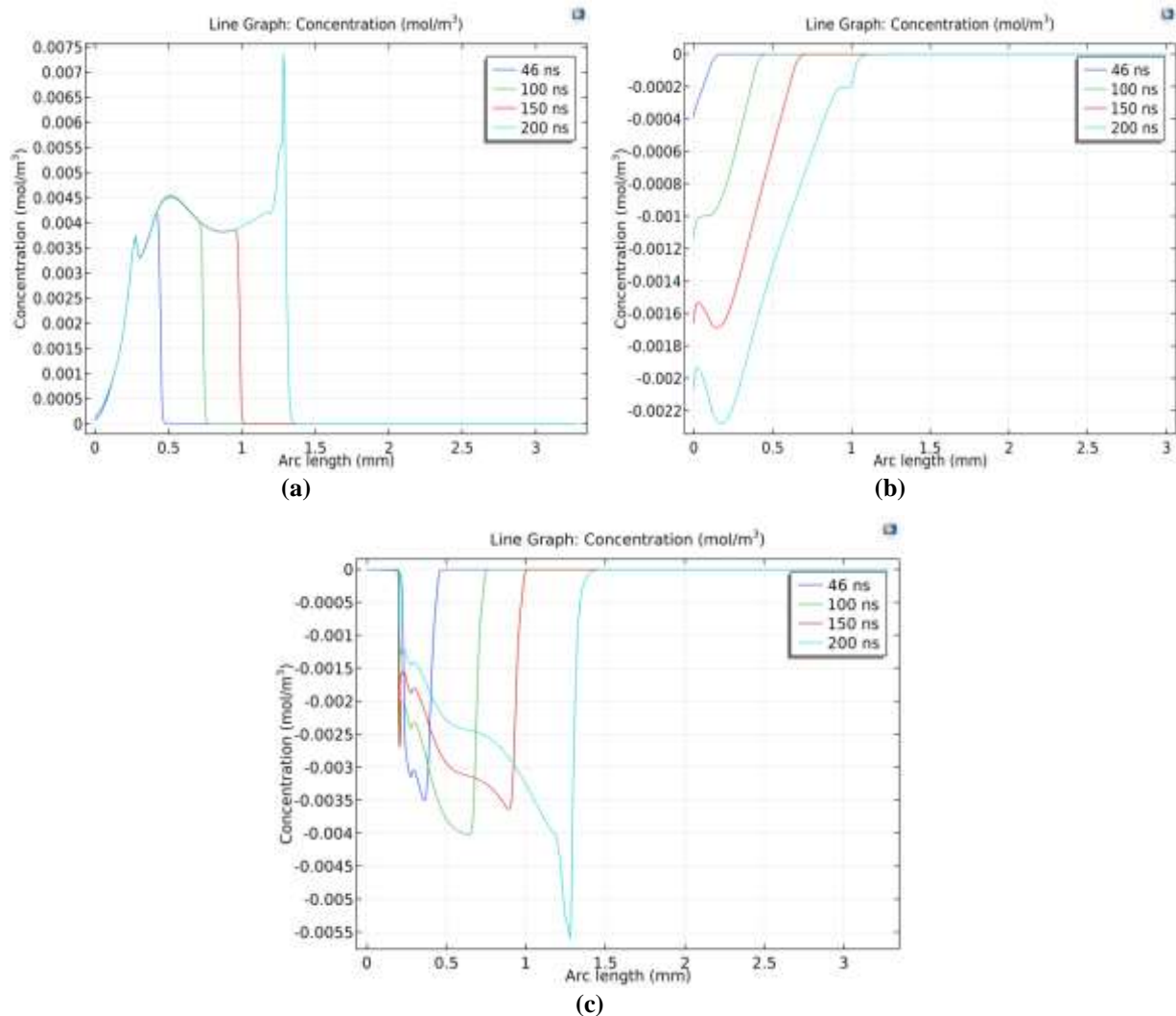


Figure 11: Distribution of charge concentrations at various times (a) positive ions (b) negative ions (c) electron density

1.4 Conclusions

In this paper, the initiation and propagation of streamer discharge was analyzed by numerical methods using COMSOL Multiphysics techniques. In accordance with the results obtained in this work, the following conclusions can be described:

- Time evaluation has an important effect on the streamer discharge propagation along the symmetry axis between the anode and cathode electrodes.
- The lowest insulator breakdown voltage was recorded at 113 kV within 200 ns.
- The highest value of streamer velocity was recorded at 5 km/s when the streamer discharge reached the plate electrode, while the lowest value was recorded at 4 km/sec when the streamer discharge starts to propagate. This is in agreement with reported results of the numerical analysis and is similar to the experimental results [27, 28].
- The behavior of space charge distribution was confirmed to be in good agreement with the value of the experimental and numerical results in previous studies [30, 31].

- Positive ions in the streamer discharge were relatively more distributed than negative ions.
- The highest electric field value was recorded at the streamer head.

Acknowledgments

The authors would like to thank the Department of Physics in University of Baghdad, Iraq.

References

- [1] H. Akiyama, "Streamer Discharges in Liquids and their Applications," *IEEE Transactions on dielectrics and electrical Insulation*, vol. 7, no. 5, pp. 646-653, 2000.
- [2] A. Sun, C. Huo, and J. Zhuang, "Formation Mechanism of Streamer Discharges in Liquids: A Review," *High Voltage*, vol. 1, no. 2, pp. 74-80, 2016.
- [3] H.-Y. Lee, J.-S. Jung, H.-K. Kim, I.-H. Park, and S.-H. Lee, "Numerical and Experimental Validation of Discharge Current with Generalized Energy Method and Integral Ohm's Law in Transformer Oil," *IEEE transactions on magnetics*, vol. 50, no. 2, pp. 257-260, 2014.
- [4] R. P. Joshi, J. F. Kolb, S. Xiao, and K. H. Schoenbach, "Aspects of Plasma in Water: Streamer Physics and Applications," *Plasma Processes and Polymers*, vol. 6, no. 11, pp. 763-777, 2009.
- [5] J. Jadidian, J. G. Hwang, M. Zahn, N. Lavesson, O. Widlund, and K. Borg, "Streamer Initiation and Propagation in Transformer Oil under Positive and Negative Impulse Voltages," in *IEEE Pulsed Power Conference*, USA, 2011.
- [6] M. N. Sadiku, "A simple introduction to finite element analysis of electromagnetic problems," *IEEE Transactions on education*, vol. 32, no. 2, pp. 85-93, 1989.
- [7] R. R. Abdulla, S. T. Ahmed, and T. H. Khalaf, "Simulation Study for the Streamer Discharge Growth within Dielectric Liquids at Solid Interface," *Iraqi Journal of Science*, vol. 49, no. 2, pp. 110-118, 2008.
- [8] O. Lesaint, A. Saker, P. Gournay, R. Tobazeon, J. Aubin, and M. Mailhot, "Streamer Propagation and Breakdown under AC Voltage in Very Large Oil Gaps," *IEEE transactions on dielectrics and electrical insulation*, vol. 5, no. 3, pp. 351-359, 1998.
- [9] D. Linhjell, L. Lundgaard, and G. Berg, "Streamer Propagation under Impulse Voltage in Long Point-Plane Oil Gaps," *IEEE transactions on dielectrics and electrical insulation*, vol. 1, no. 3, pp. 447-458, 1994.
- [10] M. Bhatt and P. Bhatt, "Effect of voltage type and polarity on streamer dynamics in transformer oil," *Materials Today: Proceedings*, 2022.
- [11] Z. Zhou, Z. Wang, W. Yan, Z. Yan, J. Wang, and Y. Geng, "Simulation Model of Streamer Discharge in Dielectric Liquid under Positive Nanosecond Pulse," in *2020 5th Asia Conference on Power and Electrical Engineering (ACPEE)*, 2020: IEEE, pp. 1933-1939.
- [12] J. Salazar, N. Bonifaci, A. Denat, and O. Lesaint, "Characterization and Spectroscopic Study of Positive Streamers in Water," in *IEEE International Conference on Dielectric Liquids*, USA, 2005.
- [13] J. Jadidian, "Charge Transport and Breakdown Physics in Liquid/Solid Insulation Systems," Ph.D. dissertation, Department of Electrical Engineering and Computer Science, Massachusetts Institute of Technology, Cambridge, MA, USA, 2013.
- [14] P. Bruggeman and C. Leys, "Non-Thermal Plasmas in and in Contact with Liquids," *Journal of Physics D: Applied Physics*, vol. 42, no. 5, p. 053001, 2009.
- [15] F. M. O'Sullivan, "A model for the Initiation and Propagation of Electrical Streamers in Transformer Oil and Transformer Oil Based Nanofluids," Ph.D. dissertation, Department of Electrical Engineering and Computer Science, Massachusetts Institute of Technology, Cambridge, MA, USA, 2007.
- [16] H. M. Y. Li, Y. Wei, G. Zhang, S. Wang, W. Zhang, Z. Li, J. Jadidian and M. Zahn, "Sub-Microsecond Streamer Breakdown in Transformer Oil-Filled Short Gaps," *IEEE Transactions on Dielectrics and Electrical Insulation*, vol. 21, no. 4, pp. 1616-1626, 2014.
- [17] J. M. Meek and J. D. Craggs, *Electrical Breakdown of Gases*. USA: Wiley, 1978, p. 878.
- [18] O. Lesaint and T. Top, "Streamer Initiation in Mineral Oil. Part I: Electrode Surface Effect under Impulse Voltage," *IEEE Transactions on Dielectrics and Electrical Insulation*, vol. 9, no. 1, pp. 84-91, 2002.

- [19] J.-W. G. Hwang, "Elucidating the Mechanisms Behind Pre-Breakdown Phenomena in Transformer Oil Systems," Ph.D. dissertation, Department of Electrical Engineering and Computer Science, Massachusetts Institute of Technology, Cambridge, MA, USA, 2010.
- [20] IEC, *Methods for the Determination of the Lightning Impulse Breakdown Voltage of Insulating Liquids*. Switzerland: IEC 60897, 1987.
- [21] H.-V. T. Techniques—Part, "1: General Definitions and Test Requirements," *IEC Standard*, pp. 60060-1, 2010.
- [22] J. Jadidian, M. Zahn, N. Lavesson, O. Widlund, and K. Borg, "Effects of Impulse Voltage Polarity, Peak Amplitude, and Rise Time on Streamers Initiated from A Needle Electrode in Transformer Oil," *IEEE Transactions on Plasma Science*, vol. 40, no. 3, pp. 909-918, 2012.
- [23] T. Briels, J. Kos, G. Winands, E. Van Veldhuizen, and U. Ebert, "Positive and Negative Streamers in Ambient Air: Measuring Diameter, Velocity and Dissipated Energy," *Journal of Physics D: Applied Physics*, vol. 41, no. 23, p. 234004, 2008.
- [24] S. Pancheshnyi, M. Nudnova, and A. Starikovskii, "Development of A Cathode-Directed Streamer Discharge in Air at Different Pressures: Experiment and Comparison with Direct Numerical Simulation," *Physical Review E*, vol. 71, no. 1, p. 016407, 2005.
- [25] Y. Li, H. Mu, J. Deng, G. Zhang, and S. Wang, "Simulation Study on Streamer Discharge in Transformer Oil under Positive Nanosecond Pulse Voltage," *Acta Phys. Sinica*, vol. 62, no. 12, pp. 124703-1, 2013.
- [26] L. Lundgaard, D. Linhjell, G. Berg, and S. Sigmond, "Propagation of Positive and Negative Streamers in Oil With and Without Pressboard Interfaces," *IEEE transactions on dielectrics and electrical insulation*, vol. 5, no. 3, pp. 388-395, 1998.
- [27] J. Jadidian, M. Zahn, N. Lavesson, O. Widlund, and K. Borg, "Abrupt Changes in Streamer Propagation Velocity Driven by Electron Velocity Saturation and Microscopic Inhomogeneities," *IEEE Transactions on Plasma Science*, vol. 42, no. 5, pp. 1216-1223, 2014.
- [28] G. Massala and O. Lesaint, "Positive Streamer Propagation in Large Oil Gaps: Electrical Properties of Streamers," *IEEE Transactions on dielectrics and electrical insulation*, vol. 5, no. 3, pp. 371-381, 1998.
- [29] D. Liu, Q. Liu, and Z. Wang, "Modelling of second mode positive streamer in cyclohexane by considering optimized electron saturation velocity," *Journal of Physics D: Applied Physics*, vol. 54, no. 11, p. 115502, 2021.
- [30] W. Sima, J. Shi, Q. Yang, S. Huang, and X. Cao, "Effects of Conductivity and Permittivity of Nanoparticle on Transformer Oil Insulation Performance: Experiment and Theory," *IEEE Transactions on Dielectrics and Electrical Insulation*, vol. 22, no. 1, pp. 380-390, 2015.
- [31] G. Chen, J. Li, Z. Huang, F. Wang, Y. Duan, and L. Dan, "Simulation of the effect of carrier density fluctuations on initial streamer branching in natural ester during pulsed positive discharges," *IEEE Transactions on Dielectrics and Electrical Insulation*, vol. 27, no. 5, pp. 1604-1610, 2020.